Contrib Mineral Petrol (2001) 141: 297–306
DOI 10.1007/s004100100253

Frank R. Schilling · Marcus Hauser
Stanislav V. Sinogeikin · Jay D. Bass

Compositional dependence of elastic properties and density of glasses in the system anorthite-diopside-forsterite

Received: 3 March 2000 / Accepted: 20 January 2001 / Published online: 11 April 2001

Abstract The compressional (v_P) and shear (v_S) wave velocities of 20 glasses in the pseudoternary system anorthite (An)–diopside (Di)–forsterite (Fo) were measured by Brillouin spectroscopy as a means of constraining the effect of composition on the elasticity of glasses. The velocity data together with measured densities were used to calculate the elastic properties: Young's modulus (E), adiabatic bulk modulus (K_S), shear modulus (G), and Poisson's ratio (σ). The data show that different chemical constituents affect the density, velocities and elastic properties in a highly systematic way. All of the properties we examined are well described by ideal mixing of molar properties. The addition of MgO strongly increases the bulk, Young's and shear moduli. The results are compared to different models describing the elastic properties of glasses as a function of chemical composition. We show that the influence of magnesia is underestimated in previous models, in some cases due to a lack of appropriate experimental data. The relatively large values of elastic moduli for magnesia-rich glasses can be explained by the high bonding strength between magnesium and SiO_4 and AlO_4 tetrahedra. The strongest effect of magnesium is on the bulk modulus; the shear modulus is less affected. Therefore, Poisson's ratio shows a modest increase with increasing MgO content. The observed increase of Poisson's ratio with increasing MgO content may be explained by a reduced bond strength between tetrahedra due to the addition of MgO.

F.R. Schilling (✉) · S.V. Sinogeikin · J.D. Bass
Department of Geology,
University of Illinois at Urbana-Champaign,
1301 W. Green St., Urbana, IL 61801, USA

M. Hauser
Institut für Mineralogie, Freie Universität Berlin,
Takustraße 6, 14195 Berlin, Germany

F.R. Schilling
Present address: GeoForschungsZentrum Potsdam,
Division 4, Telegrafenberg, 14473 Potsdam, Germany
e-mail: fsch@gfz-potsdam.de
Tel.: +49-331-2881875, Fax: +49-331-2881402

Editorial responsibility: T.L. Grove

Introduction

The density of silicate melts is an important property for describing the migration of melts in geological settings. The ascent and descent of silicate melts in the Earth's crust and mantle, stratification of magma bodies, fractionation, and partial melting processes are affected by the density contrast between melts and the surrounding solid rocks (Stolper et al. 1981; Bagdassarov et al. 1999). The high compressibility of melts as compared to minerals leads to a greater density increase with increasing depth (increasing pressure) for melts than for coexisting minerals. Therefore, the density and compressibility of noncrystalline solids are of great importance for understanding melt segregation in the crust and mantle.

Although basalts dominate hot-spot volcanism and the world's oceanic basins, few experimental data are available on the elastic properties of basaltic melts and magnesia-rich compositions. Due to the structural similarities between silicate melts and glasses (Stebbins et al. 1995), the physical properties of glasses can often be related to the physical properties of the corresponding melts. Knowledge of the properties of magnesia-rich glasses is therefore a starting point for understanding the behavior of basaltic melts.

To constrain the effect of composition on the elasticity of glasses, we measured the acoustic velocities and density of 20 different glasses in the pseudoternary system anorthite ($CaAl_2Si_2O_8$)–diopside ($CaMgSi_2O_6$)–forsterite (Mg_2SiO_4), a model basaltic system (Fig. 1). The velocity and density data were used to calculate the elastic moduli and Poisson's ratio of the glass samples. Our results show that different chemical constituents affect the elasticity of these glasses in a highly systematic way. The results are compared with models describing

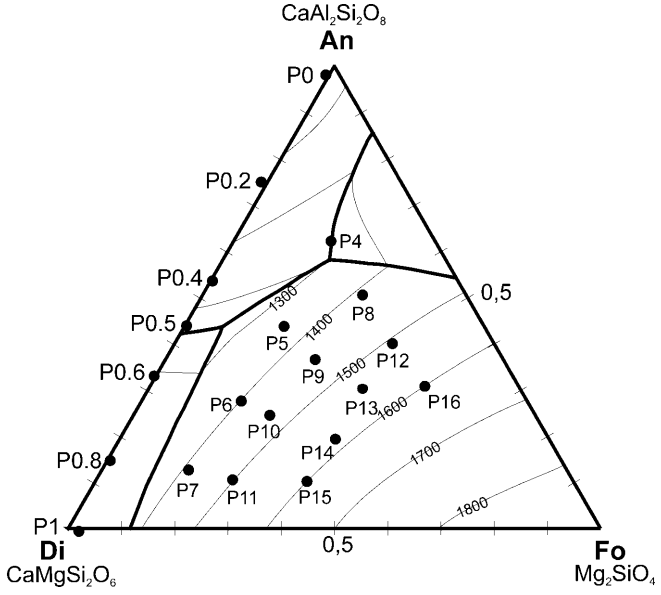

Fig. 1 Chemical composition of the glass samples in the pseudo-ternary anorthite-diopside-forsterite system. Liquidus temperatures are drawn as isotherms (modified after Hauser et al. 1998)

the elastic properties of glasses as a function of their chemical composition. Possible implications for the structure and internal forces within these amorphous materials are discussed.

Experimental

The glass samples are identical to those used for previous viscosity and electrical conductivity measurements (Hauser et al. 1998; Hauser 2000). High-purity oxide and carbonate powders were mixed and melted at 1,500–1,600 °C in Pt/Au and Pt/Rh crucibles, depending on the glass composition. To insure homogeneity of the samples, the melt was carefully stirred, and quenched in air by pouring it onto a liquid N_2-cooled Cu block. The obtained glasses were crushed, mixed, and remelted at least twice. Further details of the sample preparation are given by Hauser (2000).

Electron microprobe and X-ray fluorescence analyses were used to determine the chemical compositions (Hauser 2000; Table 1; Fig. 1). For Brillouin spectroscopy optically clear, inclusion-free samples (≈2×4 mm) were polished plane parallel to a thickness of 0.2–0.4 mm.

A schematic diagram of the experimental setup (Brillouin spectrometer) is shown in Fig. 2. We used an Ar-ion laser ($\lambda = 514.5$ nm) as a light source and a 90° symmetric scattering geometry, where the incident beam and scattering direction are at 45° to the sample surfaces. In symmetric scattering geometry on plane-parallel samples, uncertainties from the refractive index are effectively eliminated (Whitfield et al. 1976). The scattered light was analyzed with a six-pass piezoelectrically scanned Fabry-Pérot interferometer used in combination with a photomultiplier tube (PMT). Further details of the experimental setup are described by Sinogeikin et al. (1998). The velocities were determined from the mean of at least four redundant measurements in which the sample was turned by 180° to reduce possible errors caused by the deviation from an ideal scattering geometry. The system was periodically calibrated against a MgO single-crystal standard. In the experiments described here, the elastic velocities are measured in the GHz range and the reported elastic properties represent unrelaxed behavior.

Table 1 Chemical composition and corresponding anorthite, diopside and forsterite contents. The amount of nonbridging oxygen versus tetrahedron (NBO/T) is calculated from the chemical composition. For details see Hauser (2000)

	P0	P02	P04	P05	P06	P08	P1	P4	P5	P6	P7	P8	P9	P10	P11	P12	P13	P14	P15	P16
(wt%)																				
SiO_2	42.62	44.18	47.78	49.52	49.81	53.51	55.21	44.70	46.75	49.23	51.65	44.49	46.42	48.75	50.21	42.24	45.58	46.57	49.63	43.76
Al_2O_3	36.65	29.27	21.62	17.84	14.37	7.25	0.00	26.05	19.42	13.08	6.45	22.63	17.25	11.85	6.03	19.37	15.30	10.18	4.95	17.11
MgO	0.00	3.78	7.72	9.53	11.34	15.40	18.01	9.56	13.23	16.37	19.27	13.95	17.01	19.56	23.01	19.51	21.91	25.45	27.21	24.81
CaO	20.54	21.89	22.50	22.50	24.04	25.24	25.52	18.87	19.95	20.64	22.00	17.50	18.65	19.43	20.35	15.50	16.24	17.00	17.39	13.26
$\sum$	99.81	99.12	99.62	99.39	99.56	101.40	98.73	99.18	99.35	99.32	99.37	98.57	99.33	99.59	99.60	96.62	99.03	99.20	99.18	98.94
(mol%)																				
SiO_2	39.53	41.00	43.88	45.49	45.53	47.75	50.47	40.68	42.22	44.29	46.30	40.19	41.41	43.26	44.27	38.14	40.10	40.59	43.28	38.01
$AlO_{1.5}$	40.06	32.01	23.40	19.31	15.48	7.63	0.00	27.94	20.67	13.87	6.81	24.09	18.14	12.39	6.27	20.61	15.86	10.46	5.09	17.52
MgO	0.00	5.23	10.57	13.05	15.45	20.49	24.54	12.97	17.81	21.95	25.75	18.78	22.62	25.87	30.24	26.26	28.73	33.07	35.38	32.13
CaO	20.41	21.76	22.14	22.15	23.54	24.13	24.99	18.40	19.30	19.89	21.13	16.94	17.83	18.47	19.22	14.99	15.31	15.88	16.25	12.34
[mol%]																				
Anorthite	99.06	74.45	52.69	43.06	33.12	15.74	0.00	61.62	43.56	28.43	13.55	50.43	36.63	24.52	11.91	39.98	30.52	19.30	9.39	32.91
Diopside	1.88	26.79	47.01	55.69	67.63	83.91	100.90	19.54	37.80	53.14	70.49	20.48	35.37	48.58	61.18	18.19	28.38	39.31	50.60	13.46
Forsterite	–0.94[a]	–1.23[a]	0.29	1.25	–0.75[a]	0.34	–0.90[a]	18.84	18.63	18.44	15.96	29.09	28.00	26.90	26.91	41.84	41.09	41.39	40.00	53.63
NBO/T	0.01	0.30	0.62	0.79	1.02	1.47	1.96	0.51	0.85	1.20	1.64	0.74	1.05	1.37	1.83	1.05	1.29	1.71	2.03	1.29

[a]Negative forsterite content indicate that there is not enough MgO in the glass to produce stoichiometric diopside if the Al_2O_3, CaO, SiO_2 content in anorthite is stoichiometric

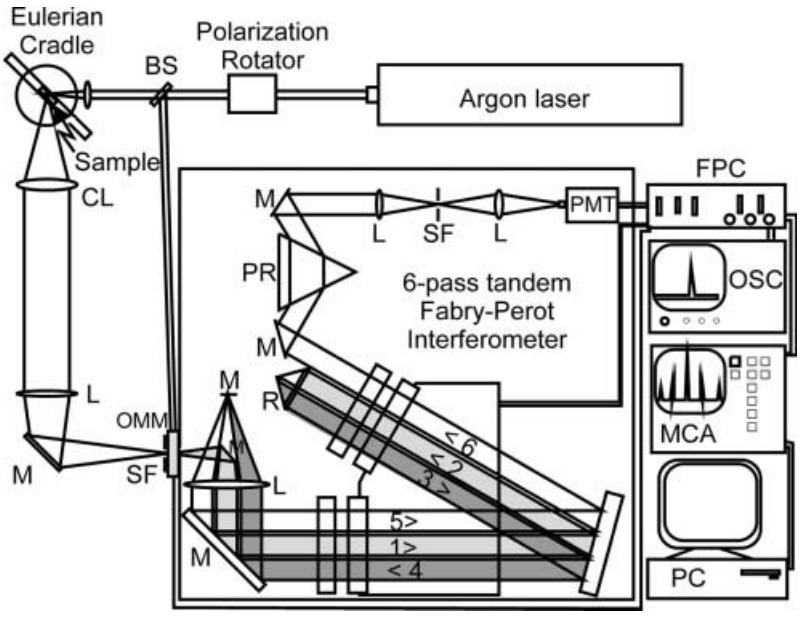

Fig. 2 Schematic diagram of the Brillouin spectrometer used (simplified from Sinogeikin et al. 1998). *BS* Beam splitter, *FL* focusing lens, *CL* collecting lens, *L* lens, *M* mirror, *OMM* optomechanical modulator, *SF* spatial filter, *R* reflector, *PR* prism, *PMT* photomultiplier tube, *FBC* Fabry-Perot controller, *OSC* oscilloscope, *MCA* multichannel analyzer, *PC* personal computer

In a symmetric 90° scattering geometry, the Brillouin shift ($\Delta\omega_i$) of a particular acoustic mode i does not depend on the refractive index of the sample. The sound velocities v_i (where v_i corresponds to v_S or v_P) were calculated according to

$$v_i = \frac{\Delta\omega_i \, \lambda}{\sqrt{2}} \tag{1}$$

where λ is the wavelength of the laser light (Whitfield et al. 1976).

To enhance signal-to-noise ratio, the recorded Brillouin spectra were filtered digitally with a low-pass Fourier filter (Fig. 3). The positions of the peaks in the Brillouin spectra were evaluated as the centers of the full width at half-maximum of the filtered peaks (Fig. 3).

The density (ρ) of each glass was measured by the Archimedean method with a Berman microbalance (Berman 1939; Table 2). The weight of samples with a mass of at least 80 mg was measured at room temperature in air and toluene, from which the density was calculated. The resultant densities are accurate to within ± 0.003 g/cm^3; the precision is even better. The accuracy was determined by use of a quartz standard ($\rho = 2.648$ g/cm^3).

Results

The elastic moduli and Poisson's ratio are calculated from the wave velocities and density using the relations:

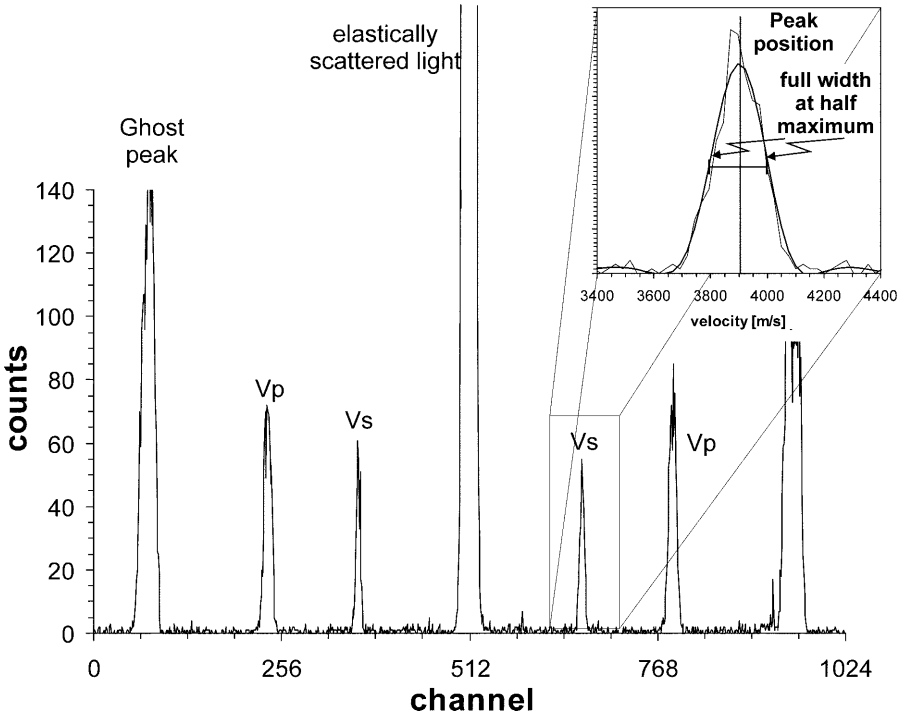

Fig. 3 Brillouin spectrum and evaluation procedure. The *inset* shows both raw spectrum and spectrum after applying a low-pass filter. The Brillouin shifts corresponding to v_P and v_S velocities are deduced as the center of the width of the filtered peak at half-maximum. The velocities are calculated according to Eq. (1)

Table 2 Velocities, density and elastic moduli, and Poisson's ratio of glasses (for details see text). The uncertainties in the acoustic velocities (2×RMS) do not exceed 1% (typically 0.7%). The uncertainty in density is ±0.003 g/cm^3, the resulting uncertainties in the elastic properties is less than 1%

	P0	P02	P04	P05	P06	P08	P1	P4	P5	P6	P7	P8	P9	P10	P11	P12	P13	P14	P15	P16
v_P (m/s)	6,695	6,676	6,683	6,697	6,723	6,721	6,739	6,787	6,808	6,783	6,787	6,898	6,886	6,884	6,886	6,960	6,966	7,012	6,967	7,046
v_S (m/s)	3,777	3,754	3,749	3,751	3,766	3,757	3,751	3,800	3,801	3,780	3,781	3,850	3,835	3,827	3,821	3,865	3,856	3,876	3,857	3,896
v_P/v_S	1.772	1.778	1.782	1.786	1.785	1.789	1.797	1.786	1.791	1.794	1.795	1.792	1.796	1.799	1.802	1.801	1.806	1.809	1.806	1.809
ρ (g/cm^3)	2.699	2.727	2.760	2.777	2.802	2.842	2.861	2.778	2.807	2.820	2.872	2.785	2.830	2.852	2.873	2.833	2.847	2.896	2.899	2.863
K_S (GPa)	69.6	70.3	71.5	72.5	73.7	74.9	76.3	74.5	76.0	76.0	77.6	77.5	78.7	79.5	80.3	80.8	81.7	84.4	83.2	84.2
K_T (GPa)	69.4	70.0	71.3	72.2	73.4	74.6	76.0	74.2	75.7	75.7	77.3	77.2	78.4	79.1	80.0	80.5	81.3	84.0	82.9	83.8
G (GPa)	38.5	38.4	38.8	39.1	39.7	40.1	40.2	40.1	40.6	40.3	41.1	41.3	41.6	41.8	42.0	42.3	42.4	43.5	43.1	43.5
E (GPa)	97.5	97.5	98.6	99.3	101.0	102.1	102.7	102.0	103.3	102.7	104.7	105.2	106.1	106.6	107.2	108.1	108.3	111.4	110.3	111.2
Poisson's ratio	0.267	0.269	0.270	0.272	0.271	0.273	0.276	0.272	0.274	0.275	0.275	0.274	0.275	0.277	0.278	0.277	0.279	0.280	0.279	0.280

[a]The isothermal bulk modulus K_T is calculated from $K_T = \frac{K_S}{1+T\alpha^2 K_S/(\rho C_P)}$, where α is the thermal volume expansivity (≈20E-6/K according to Knoche et al. 1995), and C_P is set to 800 J/(kg K) and T to 300 K. The values for K_S and ρ are taken from this study

Shear modulus	$G = v_s^2\ \rho$
Adiabatic bulk modulus	$K_s = v_\rho^2\ \rho - 4/3\ v_s^2\ \rho$
Young's modulus	$E = \frac{9K_S G}{3K_S+G}$
Poisson's ratio	$\sigma = \frac{1}{2}\left(1 - \frac{1}{(v_P/v_S)^2-1}\right) = \frac{3K_S-2G}{2(3K_S+G)}$

(2)

The velocities, densities and elastic properties are listed in Table 2. Note that the adiabatic bulk modulus K_S is systematically larger than the isothermal (K_T) modulus by a small amount (Table 2). However, the difference is smaller than the experimental error. Therefore, our discussion of systematic relationships based on K_S should also be valid for K_T, at least near ambient conditions.

When the acoustic velocities of the glasses are plotted as a function of diopside content (Fig. 4), it is seen that variation of the anorthite-diopside ratio has a minor effect on the acoustic velocities. The data suggest that the shear (v_S) velocity may decrease slightly with increasing diopside content, whereas the compressional (v_P) velocity is virtually independent of the An/Di ratio. The major feature displayed by Fig. 4 is a pronounced increase in v_P and v_S velocities with increasing forsterite content.

The minor changes in v_P and v_S with variable composition are more clearly resolved in Poisson's ratio (Fig. 5). With increasing diopside and forsterite contents, Poisson's ratio increases.

Figure 6 shows the variation of density as a function of the anorthite/diopside ratio. With increasing diopside content, an increase in density is observed. Samples with low forsterite content have lower densities than samples with high forsterite content.

Fig. 4 Longitudinal (v_p) and shear wave (v_S) velocity as a function of the diopside content. *Lines* connect samples with approximately similar forsterite (*Fo*) content. For comparison the velocities measured for glasses with anorthite and diopside compositions by Askapour et al. (1993) are indicated by *open symbols*. The mean standard deviation (*bar*) out of at least four measurements (2σ) on each sample is less than 1%

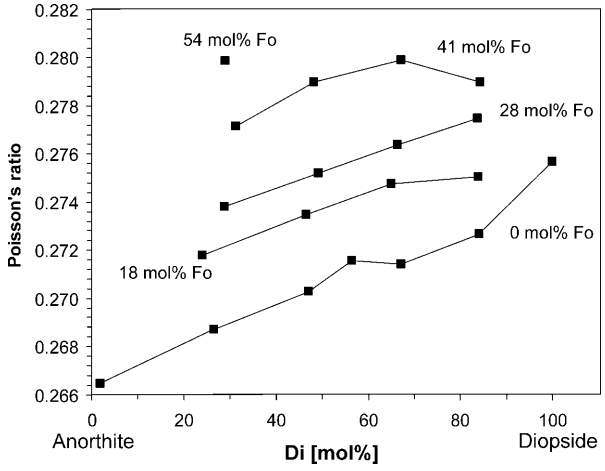

Fig. 5 Poisson's ratio versus anorthite to diopside ratio. A line connects samples with approximately similar forsterite (*Fo*) content

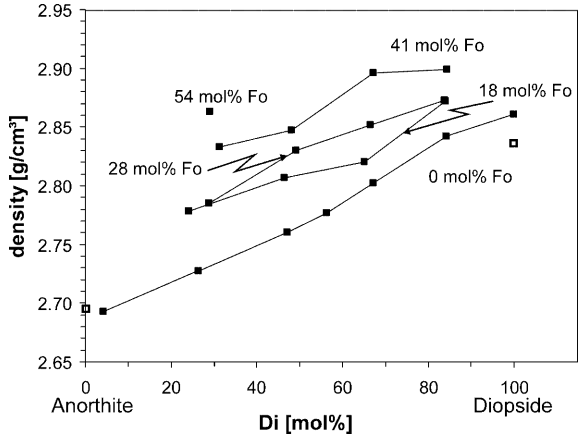

Fig. 6 Variation of the density of glasses with composition. A *line* connects samples with approximately similar forsterite (*Fo*) content. *Filled symbols* this study. *Open symbols* Askapour et al. (1993)

Discussion

General compositional trends

Density

The increase in glass density with increasing forsterite ($MgSiO_4$) and diopside ($CaMgSi_2O_6$) contents (Fig. 6) can be attributed to the increasing concentration of magnesia in the glass. This result is in accord with previous observations (Stebbins et al. 1984; Wang 1989) The molar mass of magnesium (24.3 g/mol) is much smaller than that of calcium (40.1 g/mol), but the ionic radius (Pauling radius) of magnesium (0.65 Å) is much smaller than the radius of calcium (1.14 Å). Therefore, the molar density of magnesium is higher than that of calcium, and, as a result, an increase in magnesium content leads to an increase in the density.

Velocity and Poisson's ratio

The small change observed in the v_P and v_S velocities with increasing diopside content (Fig. 4) is in good agreement with previous observations (Vo-Thanh et al. 1996). From Fig. 4 it would appear that v_P and v_S are insensitive to the Al_2O_3 content, but this inference is misleading. The influence of Al_2O_3 in isolation, and the other oxide components will be discussed below.

Although the variations in the velocities with anorthite/diopside ratio are relatively small, they result in the observed increase in Poisson's ratio with increasing diopside content (Fig. 5). Poisson's ratio is measured accurately, because it involves the ratio of v_P/v_S (Eq. 2), and any small systematic errors affecting the velocity measurements tend to cancel. The resulting uncertainty in Poisson's ratio ($\pm 0.0009 \approx \pm 0.3\%$) is calculated as the mean standard deviation from repetitive measurements on each sample. With increasing MgO/(CaO + MgO) content, the glasses show a higher Poisson's ratio (Fig. 7), as well as an increase in both the shear and bulk moduli (Fig. 8, Table 2). This is in excellent agreement with ab initio simulations (Hauser et al. 1998; Hauser 2000), which indicate that magnesium is more strongly bonded in the glass structure than is calcium.

An interesting secondary effect, which is suggested by these same simulations, is that the strength of the Si-O-Si bonds within the glass structure decreases due to the addition of magnesium (Hauser et al. 1998; Hauser 2000). This tendency to weaken the tetrahedral framework is greater for Mg than for Ca. To the extent that the shear rigidity depends on the strength of Si-O-Si bonding, MgO may increase the shear modulus G and shear velocity v_S of a glass by a lesser amount than it would in the absence of such an interaction. Therefore, v_S and G increase with the addition of MgO, but by a lesser amount than the v_P and bulk modulus, and so

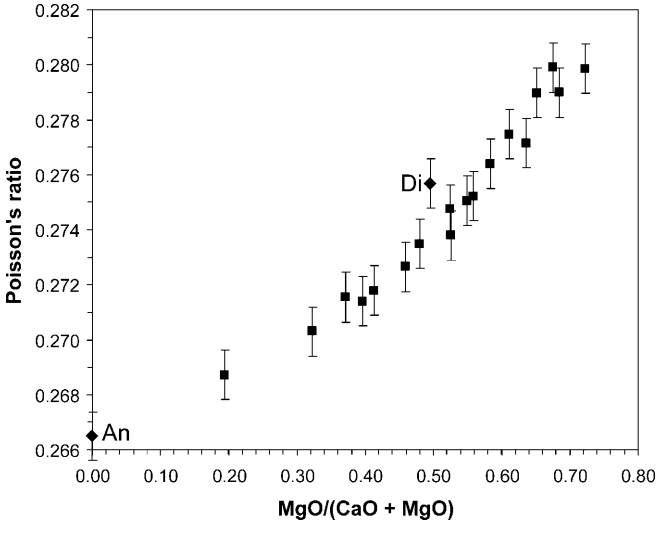

Fig. 7 Poisson's ratio as a function of the MgO content. The values of the "end-member" compositions are indicated by *An* (anorthite) and *Di* (diopside)

Poisson's ratio (Eq. 2) and the v_P/v_S ratio increase. Thus, a possible structural interpretation is that the increase in Poisson's ratio with increasing MgO content may be correlated with a reduced bonding strength between network-forming tetrahedra. Regardless, our results show that the dominant effect on the elastic properties of the glasses is the strength of Mg-O bonding, resulting in comparatively large, positive partial molar moduli.

Mixing models

Ideal molar mixing model

The elastic properties, density, and sound velocities of glasses and liquids are often expressed in terms of an ideal mixing of molar properties of oxides (e.g., Stebbins et al. 1984). A bulk property P (e.g., density, velocity, moduli) is calculated by

$$P = \sum_i x_i P_i \tag{3}$$

where x_i is the molar fraction of component i, and P_i is the corresponding molar property. These empirical molar properties can be fitted to observed data by least-square algorithms.

The elasticity and density of glasses and melts containing MgO have been measured previously (Loewenstein 1961; Soga et al. 1976; Rivers and Carmichael 1987; Wang 1989; Askapour et al. 1993; Vo-Thanh et al. 1996). Nevertheless, model calculations are heavily weighted by a small number of points representing high MgO contents. Therefore, the existing database may not suffice to accurately represent the molar properties of chemically complex high-MgO glasses.

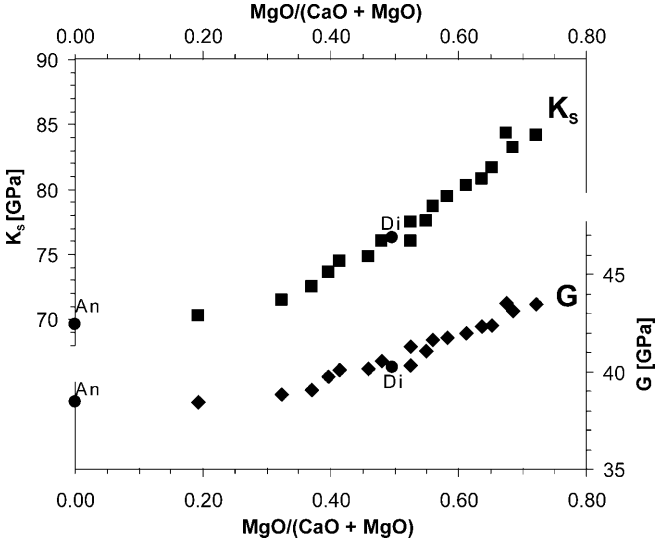

Fig. 8 Adiabatic bulk (K_S) and shear (G) modulus versus MgO content. The values of the "end-member" compositions are indicated by *An* (anorthite) and *Di* (diopside). The size of the symbols represents the experimental error

Under the assumption of an ideal mixing model (Stebbins et al. 1984; Fig. 9), molar densities were deduced from the measured values by a least-squares regression analysis (Table 3). Figure 9 shows a comparison between the measured densities and densities calculated with Eq. (3). The scatter of the data (approximately 0.003 g/cm^3) corresponds to the experimental uncertainty in the density measurements.

For the compositions examined in this study, the assumption of ideal mixing between simple oxide constituents is also satisfactory for velocities, Poisson's ratio, and elastic moduli (Figs. 10, 11, 12). As for the density, the molar velocities, moduli and Poisson's ratios (Table 3) were deduced from the measured values by a least-squares regression.

Under the assumption of a simple ionic model the molar volumes V_i, and all related properties such as the density $\rho = \sum V_i/M$ (where M is the molar mass of the glass) or the compressibility $\mathrm{d}V/\mathrm{d}P$, will mix ideally (e.g., Makishima and Mackenzie 1973). An ionic model may also explain ideal mixing of partial molar shear moduli. If ρ, K, and G mix ideally, the resultant velocities (Fig. 10) and Poisson's ratio (Fig. 11) should display nonlinear behavior (Eq. 2). However, over the restricted range of velocities and Poisson's ratios measured in this

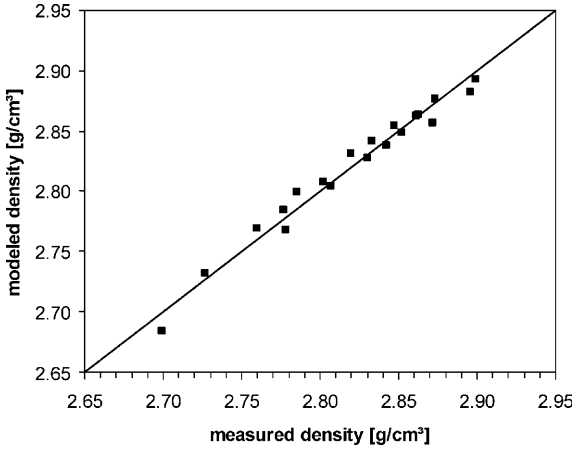

Fig. 9 Modeled versus measured density. The densities were modeled according to an ideal mixing of molar properties (Eq. 3). The scatter of the data (± 0.003 g/cm^3) corresponds to the experimental error. The *solid line* represents ideal mixing behavior. The measured and calculated densities would be equal on this line

Table 3 Molar properties of glasses in the system anorthite-diopside-forsterite. An ideal mixing law is assumed (Eq. 3)

Molar property	SiO_2	Al_2O_3	MgO	CaO
Density (g/cm^3)	2.523	2.507	3.247	3.167
v_P (m/s)	6,029	7,921	8,166	6,681
v_S (m/s)	3,419	4,421	4,369	3,791
Poisson's ratio	0.2667	0.2719	0.305	0.2602
E (GPa)	70.0	127.11	154.0	116.8
K_S (GPa)	47.4	94.5	125.2	83.8
G (GPa)	27.8	49.9	59.4	46.1

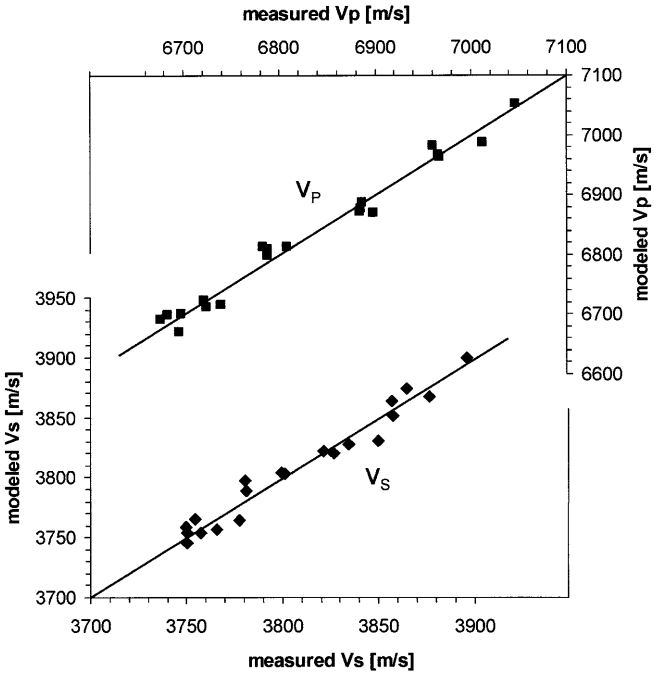

Fig. 10 Modeled versus measured v_P and v_S velocities. The velocities were calculated according to an ideal mixing of molar properties (Eq. 3). The scatter of the data is in agreement with the precision of the measurements and is smaller than $\pm 0.5\%$. The *solid line* represents ideal mixing behavior

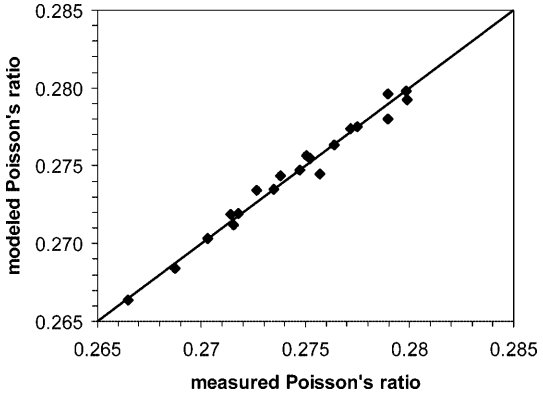

Fig. 11 Modeled Poisson's ratio as a function of the measured one (Eq. 3, Table 3). The *solid line* represents ideal mixing behavior

study, we find empirically that an ideal mixing approximation describes the observations well, even if it cannot be valid over a larger compositional range, and despite the fact that there is no theoretical basis for applying ideal mixing to nonvolumetric properties such as velocities. Additional empirical justification for our approach is provided by the results of Rivers and Carmichael (1987) who obtained partial molar velocities for the oxide constituents of silicate melts. These authors similarly cautioned against extrapolating the results of such an analysis far from the compositional range of their experiments.

SiO_2 and Al_2O_3 have similar molar densities (2.523 and 2.507 g/cm^3, respectively) but the molar moduli,

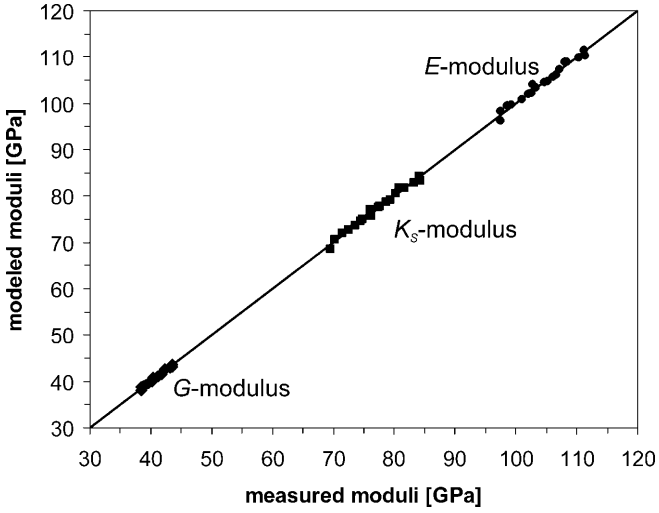

Fig. 12 Modeled G, K and E moduli compared to measured ones. The moduli were calculated according to an ideal mixing of molar properties (Eq. 3, Table 3). The scatter of the data is in agreement with the precision of the modulus determination and is smaller than $\pm 1\%$. The *solid line* represents ideal mixing behavior

compressional velocity and shear velocity of Al_2O_3 are much higher than the corresponding molar properties of SiO_2 (Table 3). As discussed above, MgO (3.247 g/cm^3) shows a higher molar density than CaO (3.167 g/cm^3). The molar moduli and velocities of MgO are much higher than those of CaO (Table 3). The minor changes in v_P and v_S velocities with variable anorthite to diopside ratio (Fig. 4) are the result of the Al_2O_3 to MgO exchange in this pseudobinary system, whereas both oxides have comparable molar velocities (Table 3). The higher $(MgO + Al_2O_3)/(CaO + SiO_2)$ ratio with increasing forsterite content leads to the observed increase in v_P and v_S, in which MgO and Al_2O_3 have higher molar velocities than CaO and SiO_2 (Table 3).

Structural related models

Makishima and Mackenzie (1973) presented a structure-based mixing model by taking into account the dissociation energy of the oxide constituents per unit volume and the packing density. Their theoretical model is based on ideal ionic bonding within the structure. These authors assume that the Young's modulus (E) of a crystalline or noncrystalline solid is given by

$$E = 2\frac{\alpha U}{r_0^3} \tag{4}$$

where α is a Madelung constant, U is the attractive electrostatic energy, and r_0 the interatomic distance. In a disordered glass structure the Madelung constant is not well defined. Makishima and Mackenzie (1973) considered the product of the dissociation energy per unit volume G_t and a relative packing density V_t instead of the Madelung constant. The packing density V_i for each oxide component Me_xO_y is linked to the Pauling ionic

radius of the component (Makishimna and Mackenzie 1973). The Young's modulus in the Makishima and Mackenzie model is expressed by

$$E = 2\frac{\rho}{M} D_t V_t$$
$$E = 2\frac{\rho}{M} \sum_i D_i x_i \sum_i V_i x_i \quad (5)$$

where D_i is the molar dissociation energy, ρ is the bulk density, and x_i the molar fractions.

The Makishima and Mackenzie model was extended by Rocherulle et al. (1989) to describe the elastic moduli of high-strength glasses, especially oxynitride glasses. They modified the packing density by an additional parameter Z – the number of formula units per "unit volume" (referred as "unit cell" by Rocherulle et al. 1989) – which is fitted to the data.

Following the model of Rocherulle et al. (1989), the Young's modulus is expressed as

$$E = 2\sum_i G_i x_i \sum_i C_i x_i \quad (6)$$

where $C_i = V_i(\rho/M)Z$ is the packing factor.

The bulk modulus K_S is approximated in both models by a linear relationship between K and E.

$$K = \beta V_t E \quad (7)$$

with $\beta = 1.2$ for the Makishima and Mackenzie model and 1.08 for the modified model of Rocherulle et al. (1989). The latter authors used a slightly different G_i value for alumina than Makishima and Mackenzie (1973). The G_i, V_i, and C_i values for both models are listed in Table 4.

Elastic properties

In Fig. 13 the measured elastic properties are compared to the theoretical model of Makishima and Mackenzie (1973), Rocherulle et al. (1989), and the empirical relation (ideal mixing Eq. 3) by Wang (1989). A better correlation between the measured and modeled E moduli is observed for glasses with low magnesia content (anorthite dominated). With increasing forsterite and diopside (Mg) contents, deviations between modeled and observed E moduli increase. Therefore, the influence of magnesium on the strength of glasses is underestimated in all three models.

Table 4 G_i, V_i, and C_i values for the models after Makishima and Mackenzie (1973), and Rocherulle et al. (1989). *Value in parentheses* G_I value used by Rocherulle et al. (1989)

Compound	G_i (mJ/m^3)	V_i (mm^3)	C_i
SiO_2	64.4	14.0	0.6174
Al_2O_3	133.8 (120)	21.4	0.8333
CaO	63.8	9.4	0.5530
MgO	83.6	7.6	0.6750

The deviation (Fig. 14) between observed and modeled values – calculated using the ideal mixing approach and the data set of Wang (1989) – can be attributed to the lack of appropriate data for magnesia-rich compositions. The older data (Loewenstein 1961; Soga et al. 1976; Wang 1989) underestimate the effect of magnesia on the E modulus (Table 3).

The increasing discrepancy for glasses with increasing ionic strength (high magnesia content) is plotted in Fig. 14 as a function of the number of **n**on**b**ridging **o**xygens divided by the number of ($SiO_4 + AlO_4$) **t**etrahedra (NBO/T). The NBO/T ratio is not independent of the magnesia content in the system. Therefore, two explanations are possible to interpret the observations. The deviation between the measured and modeled E modulus might result from the increasing number of NBO/T. This would imply that the higher strength of these glasses compared to the calculated value is due to the lower degree of polymerization. On the other hand, depolymerization – disruption of the framework – leads

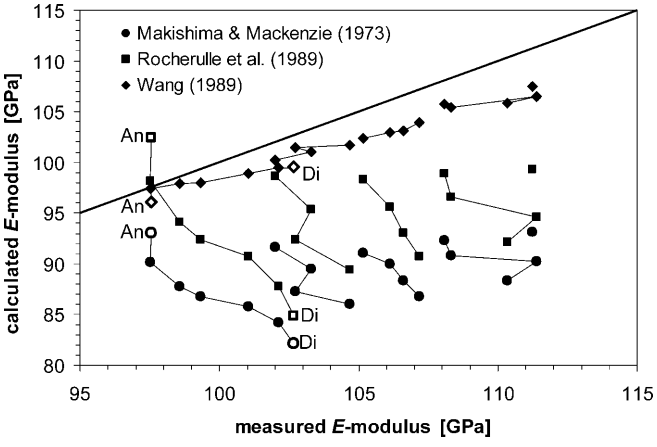

Fig. 13 Measured E modulus compared to moduli calculated from different models. The solid line represents an ideal model, where measured and calculated E modulus would be equal

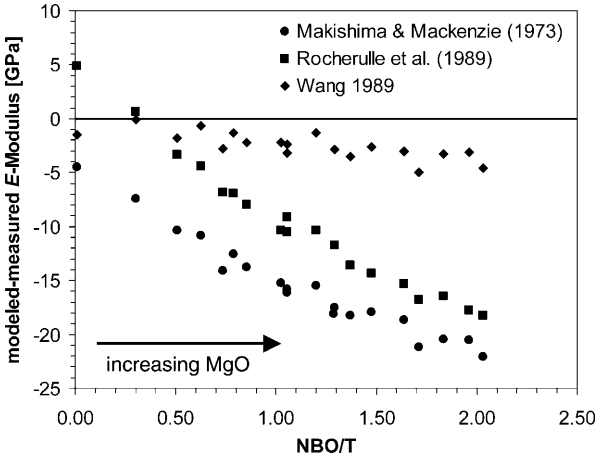

Fig. 14 Difference between measured and calculated E moduli as a function of the number of nonbridging oxygen divided by the number of tetrahedra (NBO/T)

to a decrease in the fraction of strong bonds between tetrahedra and, therefore, should lead to a lower Young's modulus, which is in contradiction to the observation (Fig. 14). Makashima and Mackenzie (1973) and Rocherulle (1989) showed for various compositions with variable NBO/T that the ionic models work fine for alkaline glasses and even for oxynitride glasses, independent of the NBO/T ratio. Therefore, the assumption of a dominating influence of NBO/T to Young's modulus cannot explain the observed behavior.

If we assume that the difference in strength between modeled and measured properties is due to the increased magnesia content, we can conclude that the influence of magnesium on the strength of the glass is underestimated and that MgO has a significant influence on the structure of the glass.

Because all of the glasses we studied are transparent and poor electrical conductors, metallic bonding in these glasses may be neglected. As pointed out above, molecular simulations indicate strong bonding of magnesium to the adjacent clusters of tetrahedra. Similar to the explanation for AlN components in glasses (Rocherulle et al. 1989), the difference between the observed and measured E modulus may be explained by a higher strength of Mg^{++}-related bonds compared to simplified ionic models. This is in good agreement with the result of ab initio simulations (Hauser et al. 1998; Hauser 2000), which show that Mg^{2+} is more strongly bonded within the glass structure than is Ca^{2+}. This can be taken into account in the ionic model of Rocherulle et al. (1989) by an increased packing density and, therefore, higher Z value for MgO. An increase in the observed E-modulus with increasing magnesia content can thus be explained by increasingly stronger bonding and a resultant higher packing density due to magnesium ions. In other words, MgO does fundamentally change the structure.

Our results indicate that an extrapolation of molar properties to vastly different chemical compositions may result in a significant error (Fig. 14, high MgO-contents). As the glass structure may strongly depend on different constituents, the use of molar properties over a wide range of composition could be misleading. This is clearly demonstrated by silica glass, for which the inferred molar density (2.523 g/cm^3), K_S (47.4 GPa), and G (27.8 GPa) of a virtual SiO_2 component compare poorly with the measured values for silica glass ($\rho = 2.204$ g/cm^3; $K_S = 36.5$ GPa; $G = 31.2$ GPa; values taken from Bass 1995).

Due to the structural similarities between silicate melts and glasses (Stebbins et al. 1995), the physical properties of glasses can often be related to the physical properties of the corresponding melts. We speculate that the pronounced but often underestimated influence of MgO on the elastic properties of glasses should also be valid at higher temperatures (e.g., for basaltic melts), although the magnitude of such an effect may be different in actual melts. The observed strong bonding of Mg within the glass structure should cause an increase in the elastic moduli with increasing MgO content for melts as well. Due to the stronger bonding, lower temperature and pressure derivatives of the elastic moduli would be expected. The limited database for glasses with high MgO content already shows a strong influence of MgO on the elastic properties (e.g., Stebbins et al. 1995). Marginal support for this model comes from the results of Rivers and Carmichael (1987) who found that the molar $(dV/dP)_T$ for MgO is approximately zero for silicate melts, although the value of this property was generally small for most of the oxide constituents. Additional support comes from the results of Lange (1997) who found a smaller molar $(dV/dT)_P$ for MgO compared to other alkaline or earth-alkaline oxides for silicate melts.

Therefore, all inferences about the behavior of basaltic melts which are based on the properties of MgO-poor melts may need to be reevaluated. If MgO-rich melts have lower temperature and pressure derivatives of elastic properties, then basic or ultrabasic melts would experience a larger buoyancy force at depth due to pressure, but a smaller buoyancy force due to the high temperatures of the interior. Which of these effects will dominate is uncertain. Because the pressure and temperature derivatives of basaltic melts are rarely known, all models that include the buoyancy forces of basaltic melts are highly speculative. Therefore, this study on the elastic properties of glasses can only be the starting point of a more detailed study of the elastic properties at elevated temperatures and pressures.

As the velocity and elasticity systematics of basaltic melts are fairly uncertain, conclusions drawn from extrapolated elastic properties for basaltic melts may be misleading. Therefore, systematic investigations are necessary to understand in more detail the elastic and rheological properties of basaltic melts at elevated temperatures. Atomic-level simulations and spectroscopic investigations could give additional information.

Acknowledgements We express our gratitude to Prof. Dr. J. Arndt for the support of this work. The helpful and constructive comments of two anonymous reviewers are gratefully acknowledged. Financial support from the Deutsche Forschungsgemeinschaft (grant SFB 267 "Deformation processes in the Andes", Heisenberg grant Schi545/1) and the National Science Foundation is gratefully acknowledged.

References

Askapour V, Manghnani MH, Richet P (1993) Elastic properties of diopside, anorthite, and grossular glasses and liquids: a Brillouin scattering study up to 1400 K. J Geophys Res 98(B10):17683–17689

Bagdassarov N, Laporte D, Thompson AB (1999) Physics and chemistry of partially molten rocks. Kluwer, Dordrecht

Bass JD (1995) Elasticity of minerals, glasses and melts. In: T.J. Ahrens (ed) Mineral physics and crystallography: a handbook of physical constants. AGU Ref Shelf 2:45–63

Berman H (1939) Torsion microbalance for the determination of specific gravities of minerals. Am Mineral 24:434–438

Hauser M (2000) Struktur und Dynamik unterkühlter basaltischer Schmelzen. Berliner Geowissenschaftliche Abhandlungen, A 206

Hauser M, Arndt J, Schilling FR, Cordes F (1998) Structure and transport properties of basaltic melts. Ber Dtsch Mineral Gesell Beih Eur J Mineral 10:121

Knoche R, Dingwell DB, Webb SL (1995) Melt densities for leucogranites and granitic pegmatites: Partial molar volumes for SiO_2, Al_2O_3, Na_2O, K_2O, Li_2O, Rb_2O, Cs_2O, MgO, CaO, SrO, BaO, B_2O_3, P_2O_5, Fe_2O_{-1}, TiO_2, Nb_2O_5, Ta_2O_5, and WO_3. Geochim Cosmochim Acta 59:4645–4652

Lange RA (1997) A revised model for the density and thermal expansivity of K_2O-Na_2O-CaO-MgO-Al_2O_3-SiO_2 liquids from 700–1900 K: extension to crustal magmatic temperatures. Contrib Mineral Petrol 130:1–11

Loewenstein KL (1961) Studies in the composition and structure of glasses possessing high Young's moduli. Phys Chem Glass 2(3):69–82

Makishima A, Mackenzie JD (1973) Direct calculation of Young's modulus of glass. J Non-Cryst Solids 12:35–41

Rivers ML, Carmichael ISE (1987) Ultrasonic studies of silicate melts. J Geophys Res 92(B9):9247–9270

Rocherulle J, Eclivet C, Poulain M, Verdier P, Laurent Y (1989) Elastic moduli of oxynitride glasses: extension of Makishima and Mackenzie's theory. J Non-Cryst Solids 108:187–193

Sinogeikin SV, Katsura T, Bass JD (1998) Sound velocities and elastic properties of Fe-bearing wadsleyite and ringwoodite. J Geophys Res 103(B9):20819–20825

Soga N, Yamanaka H, Kunugi M (1976) Elastic properties and structure of alkaline-earth silicate glasses. J Non-Cryst Solid 22:67–76

Stebbins LF, Carmichael ISE, Moret LK (1984) Heat capacities and entropies of silicate liquids and glasses. Contrib Mineral Petrol 86:131–148

Stebbins JF, McMillan PF, Dingwell DB (1995) Structure, dynamics and properties of silicate melts. Mineral Soc Am Reviews in Mineralogy 32

Stolper E, Walker D, Bradford HH, Hays JF (1981) Melt segregation from partially molten source regions: The importance of melt density and source region size. J Geophys Res 86(B7):6261–6271

Vo-Thanh D, Polian A, Richet P (1996) Elastic properties of silicate melts up to 2350 K from Brillouin scattering. Geophys Res Lett 23(5):423–426

Wang H (1989) Elasticity of silicate glasses. PhD Thesis, University of Illinois at UC

Whitfield CH, Brody EM, Bassett WA (1976) Elastic moduli of NaCl by Brillouin scattering at high pressure in a diamond anvil cell. Rev Sci Instrum 47:942–947